Dalton Transactions

ROYAL SOCIETY OF CHEMISTRY

PAPER

View Article Online
View Journal | View Issue

Cite this: *Dalton Trans.*, 2024, **53**, 13815

Gastric stability of bare and chitosan-fabricated ferritin and its bio-mineral: implication for potential dietary iron supplements†

Rohit Kumar Raut, Gargee Bhattacharyya and Rabindra K. Behera *

Iron deficiency anaemia (IDA), the most widespread nutritional disorder, is a persistent global health issue affecting millions, especially in resource-limited geographies. Oral iron supplementation is usually the first choice for exogenous iron administration owing to its convenience, effectiveness and low cost. However, commercially available iron supplementations are often associated with oxidative stress, gastrointestinal side effects, infections and solubility issues. Herein, we aim to address these limitations by employing ferritin proteins—self-assembled nanocaged architectures functioning as a soluble cellular iron repository—as a non-toxic and biocompatible alternative. Our *in vitro* studies based on PAGE and TEM indicate that bare ferritin proteins are resistant to gastric conditions but their cage integrity is compromised under longer incubation periods and at higher concentrations of pepsin, which is a critical component of gastric juice. To ensure the safe delivery of encapsulated iron cargo, with minimal cage disintegration/degradation and iron leakage along the gastrointestinal tract, we fabricated the surface of ferritin with chitosan. Further, the stoichiometry and absorptivity of iron-chelator complexes at both gastric and circumneutral pH were estimated using Job's plot. Unlike bipyridyl, deferiprone exhibited pH dependency. *In vitro* kinetics was studied to evaluate iron release from bare and chitosan-fabricated ferritins employing both reductive (in the presence of ascorbate and bipyridyl) and non-reductive (direct chelation by deferiprone) pathways to determine their bio-mineral stabilities. Chitosan-decorated ferritin displayed superior cage integrity and iron retention capability over bare ferritin in simulated gastric fluid. The ability of ferritins to naturally facilitate controlled iron release in conjugation with enteric coating provided by chitosan may mitigate the aforementioned side effects and enhance iron absorption in the intestine. The results of the current study could pave the way for the development of an oral formulation based on ferritin-caged iron bio-mineral that can be a promising alternative for the treatment of IDA, offering better therapeutic outcomes.

Received 25th June 2024,
Accepted 22nd July 2024

DOI: 10.1039/d4dt01839g

rsc.li/dalton

Introduction

As reported by the World Health Organization (WHO), nearly 1.8 billion people worldwide suffer from anaemia, and about 50% of these cases are related to iron deficiency anaemia (IDA).[1,2] IDA results from persistent negative physiological iron balance in the body. Despite the availability of iron in copious amounts throughout the Earth's crust,[3,4] IDA is remarkably common in humans.[5,6] It is one of the most widespread pathological states/conditions, accounting for as much as ~20% of all nutritional disorders.[2] Blood loss, chronic diseases, parasitic infections, *etc.* are a few factors that can contribute to iron deficiency, but insufficient content of iron in the diet still remains the primary cause of IDA.[1,6] The baffling enigma of the persistence of IDA as the most prevalent anaemic and nutritional disorder in spite of the availability of a multitude of effective treatment/diagnostic procedures makes it a cause of concern.[2,7]

Iron supplementation takes the centre stage among the current strategies aimed towards the treatment, prevention, and mitigation of IDA.[2] However, the existing iron supplements are mainly inorganic iron salts or complexes (such as ferrous sulphate, ferrous gluconate, and ferrous ascorbate) taken in the form of "Fe^{2+} burst", which are commonly associated with several negative side effects.[4,8] The shift in pH from the stomach (pH ~1.5–3.0) to the intestine (pH ~6.5–7.5) along with the presence of reducing agents may trigger redox cycling of iron ($Fe^{2+} \leftrightarrow Fe^{3+}$), which can generate reactive

Department of Chemistry, National Institute of Technology, Rourkela – 769008, Odisha, India. E-mail: beherarabi@nitrkl.ac.in; Fax: +91-661-2462651; Tel: +91-661-2462980

† Electronic supplementary information (ESI) available. See DOI: https://doi.org/10.1039/d4dt01839g

oxygen species (ROS) *via* the Fenton reaction, leading to inflammation and cell damage in the digestive tract.[8] Under physiological conditions, free Fe^{3+} is almost insoluble (solubility ~10^{-18} M) and gets precipitated as Fe^{3+} oxide/hydroxide (rust), which makes absorption difficult.[3] Furthermore, anti-nutrients such as phytates and polyphenols in plant based diets are known to trap free/chelatable iron (forming complexes), ultimately lowering the amount of iron available for intestinal absorption. These stable iron complexes are then excreted out, leading to the loss of bioavailable iron.[9] Moreover, readily available exogenous free iron may also be captured by pathogenic bacteria, leading to unfavourable consequences.[10–12] Therefore, designing effectual supplementation strategies for iron are trickier than that for most other micronutrients.[13]

In physiological systems, this Fe^{2+} induced toxicity and Fe^{3+} precipitation are mitigated by sophisticated molecular machinery to meet cellular iron demands. Ferritin, a naturally occurring ubiquitous protein, presents one of those machineries.[14,15] This self-assembled nano-caged protein is the primary intracellular iron repository, capable of holding up to ~4500 Fe per cage and is critical to iron homeostasis.[16–19] It scavenges and buffers the cellular iron pool while concentrating iron in the form of a hydrated nano-particulate ferric oxyhydroxide mineral ($nFe_2O_3{\cdot}xH_2O$) in its central hollow nanocavity.[14,20–22]In recent years, ferritin nanocages have been extensively exploited in catalysis[23–25] and nano-biotechnology (as targeted drug delivery systems/imaging agents).[15,20,26–32] It is evident that human H and L ferritins naturally internalise into the cell through receptor-mediated endocytosis *via* membrane receptors like transferrin receptor-1 (TfR-1) and SCARA 5, respectively.[33–36]

In the context of ferritins being utilized as dietary iron supplements, iron loaded phytoferritins (mostly soy-ferritins) have been previously explored as a natural alternative for safer iron delivery and this protein encapsulated nano-formulation is less prone to redox recycling and less accessible to pathogens.[37–41] However, it was observed that phytoferritins cannot withstand gastric conditions (low pH and pepsin activity).[42,43] Further, molecular dynamics simulations on human ferritins showed enhanced iron mobilization under acidic conditions.[44] In this work, we propose bullfrog M ferritin, an amphibian protein caged bio-mineral, as a potential iron supplement. The rationale behind the choice of frog M ferritin lies in the fact that (i) it has a striking resemblance with human H-ferritin (structure–function homology with ~70% sequence identity) (Fig. S1†);[15,45] (ii) M ferritin protein cages are very stable, both thermally (T_m > 80 °C) and chemically (up to 5 M Gdn·HCl/7 M urea),[15] and are capable of sustaining their cage structure up to a pH of 2.0;[46,47] (iii) it is a well-studied/characterized protein often used as a model system in terms of structural and functional aspects in lieu of H-ferritin;[48–50] and (iv) M ferritins are capable of storing about 4500 atoms of iron in their soluble form, without getting precipitated.[18,51] Moreover, bullfrog meat is consumed in various parts of the world as a rich source of protein.[52,53]

For potential oral iron supplementation, the stability of the ferritin cage under the gastric conditions (while passing through the gastrointestinal tract) is a primary requirement. The ferritin proteins must retain their cage integrity and the encapsulated iron bio-mineral until they reach the intestinal cells (enterocytes) where they would be internalized/absorbed through receptor-mediated endocytosis like H-chain ferritin possibly *via* transferrin receptors (TfR-1/TfR-2). As per earlier reports, frog M ferritins can retain their cage integrity under gastric pH (pH > 2.0).[46,47] However, the cage integrity/stability might be compromised when they encounter the gastric environment due to the presence of pepsin (protease enzyme). Therefore, investigation of gastric stability of bare frog M ferritins is necessary. We hypothesize that providing an enteric coating (biopolymers) to these iron loaded ferritins would further provide better resistance against the activity of pepsin for a longer period (Fig. 1). As a result, the amount of iron release/leakage into the stomach will be minimal and the intact ferritin cage loaded with iron would reach the intestine for efficient uptake.

Chitosan is a natural cationic polysaccharide biopolymer ($-NH_2$ group with a pK_a of 6.3) that has excellent biocompatibility, better biodegradability, non-toxicity, and antibacterial properties.[54–56] These properties of chitosan have made it a Food and Drug Administration (FDA) approved food additive agent.[55] It is a versatile biological polymer that has a high number of primary amines, and these amines are a core component of chitosan's functional properties that make the polymer ideal for use in bio-fabrication applications.[54] Chitosan-fabricated nanomaterials have been extensively used historically for several drug delivery applications to minimize the unwanted leakage of cargo from carriers and non-targeted/non-specific delivery of cargo materials.[57,58] Therefore, chitosan can be used to fabricate the ferritin surface (pI ~5.6) to preserve its cage assembly and iron retention ability in the stomach environment. As pK_a values are environment dependent, interactions with chitosan (ammonium ions $-NH_3^+$) can potentially lower the pK_a values of carboxylate residues in ferritin. For example, the average pK_a values of side chains of glutamate and aspartate residues in free amino acids/small peptides are ~4.2 and ~3.5, respectively, but based on the protein environment these pK_a values can shift to as low as 2.1 (for glutamate) and 0.5 (for aspartate).[59] Additionally, chitosan's NH_3^+ groups may experience a pK_a shift when interacting with the negatively charged residues of ferritin. Under gastric conditions, in addition to the electrostatic interactions (between the positively charged NH_3^+ of chitosan and negatively charged residues on ferritin), other non-covalent interactions such as H-bonding and hydrophobic interactions could contribute to the formation of the chitosan–ferritin complex.

This report aims to explore the stability of bare and chitosan-decorated M ferritins against gastric conditions to develop a potential dietary iron supplement. Our native PAGE (poly acrylamide gel electrophoresis) and transmission electron microscopy (TEM)/dynamic light scattering (DLS) data collectively concludes that bare ferritin itself is quite resistant to the gastric environment and fabrication with chitosan further

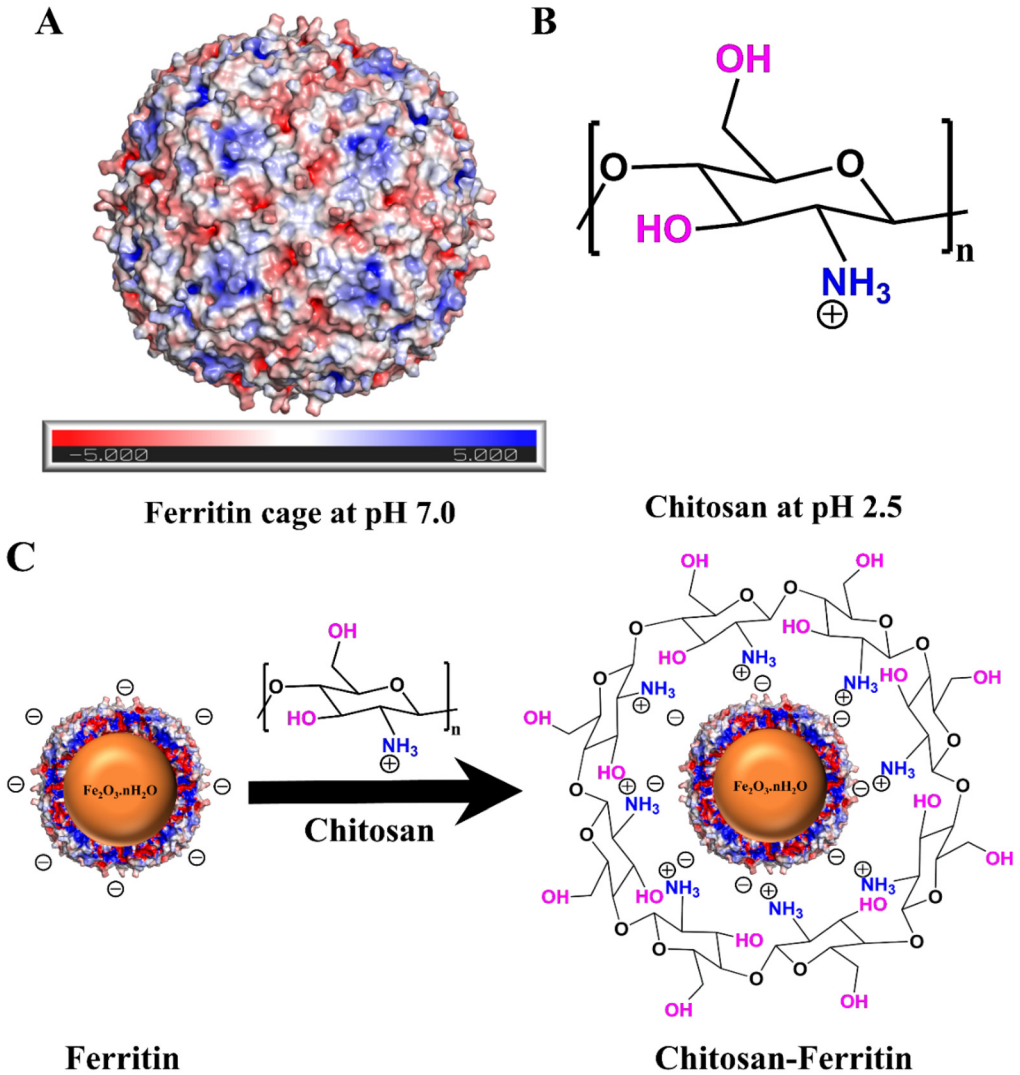

Fig. 1 Schematic representation of the fabrication of ferritin protein with chitosan. (A) Surface electrostatics of the frog M ferritin nanocage (PDB: 1MFR). Blue, white and red patches represent the presence of acidic, neutral and basic amino acid residues, respectively. (B) Skeletal structure of the chitosan biopolymer. (C) Schematic illustration of the slice of ferritin fabricated with chitosan, showing its nanocage and caged iron mineral. The over simplified ferritin–chitosan interactions may not correspond to the true/exact nature of these non-covalent interactions existing under experimental conditions. The electrostatic potential is expressed in the units of $\pm 5K_BT/e$ using the APBS tool embedded in PyMOL.

extended the stability of both apo and mineralized ferritin and prevented degradation and retained the caged iron mineral. Using zeta potential analysis, fluorescence and circular dichroism (CD) spectroscopy, the interaction between ferritin and chitosan was further validated. In reductive and non-reductive iron mobilization experiments under gastric conditions, it was observed that chitosan can minimize the iron leakage even in the presence of reducing agents and chelators. Based on our findings, ferritin decorated with chitosan has been shown to be more stable in gastric fluid when compared to ferritin alone. Therefore, the results obtained from the current work hold future implications for the engineering of acid-stable, biocompatible iron loaded frog M ferritin proteins to combat the side effects associated with the currently used commercial iron supplements.

Experimental section

Overexpression, purification, and quantification of recombinant frog M-ferritin protein

Recombinant wild type (WT) bullfrog M-ferritin protein was overexpressed in *Escherichia coli* [BL21(λDE3) pLysS] as per our previous reports.[46,48] BL21(λDE3) pLysS cells were transformed with the pET-3a vector, containing the gene for WT frog M ferritin, and cultured in lysogeny broth (LB) medium with ampicillin (100 μg mL^{-1}) as the antibiotic. WT frog M ferritin was over-expressed by isopropyl 1-thio-β-D-galactopyranoside (IPTG, 0.5 mM final concentration) induction. Following our previously established protocols, harvested cultured cells were sonicated, and centrifuged and the supernatant was processed for protein purification. Briefly, this purification process

involves heat shock (60 °C, 15 min), ammonium sulphate precipitation (65%), and dialysis followed by anion exchange chromatography (Q Sepharose fast-flow column) with 0–1 M NaCl gradient. Protein fractions were identified using sodium dodecyl sulfate–polyacrylamide gel electrophoresis (SDS–PAGE). The purified protein fractions were concentrated in an ultra-centrifugal unit with a membrane cut off of 30 kDa and buffer exchanged with 100 mM 3-(*N*-morpholino) propane sulfonic acid (MOPS) (pH 7.0) containing 100 mM NaCl. Protein concentrations were estimated by Bradford assay. Iron content in the as-purified frog M ferritin proteins was found to be ~7–10 Fe/cage, by ferrozine assay, which are referred to as 'apo' form.[18,60]

Preparation of mineralized ferritin proteins

Freshly prepared $FeSO_4$ solution (in 1 mM HCl) was added to ~1 mg mL^{-1} of as purified frog M ferritin (2.08 μM cage) in 100 mM MOPS buffer (pH 7.0) containing 100 mM NaCl as reported earlier.[18,60] The resulting solution was then incubated for 2 hours at room temperature and then overnight at 4 °C. Two sets of mineralized ferritins were prepared with the final iron concentrations maintained at 1 mM (~480 Fe/cage) and 2 mM (~960 Fe/cage). The 480 Fe/cage mineralized ferritin sample was used for iron release experiments, while 960 Fe/cage samples were used for native PAGE and TEM analysis.

Preparation of the ferritin–chitosan complex

Apo and mineralized frog M ferritin protein (concentrated 10 times by a protein concentrator with 10 kDa cut-off, Millipore) solutions were prepared in 100 mM MOPS-NaCl (pH 7.0). Chitosan (~50 kDa, Sigma) solutions were prepared by dissolving it in 100 mM Gly-HCl buffer (pH 2.5). These concentrated apo and mineralized ferritins were mixed with the chitosan solution at specific ratios (from 1 : 1 to 1 : 4 w/w of ferritin : chitosan) and the mixture (pH ~3.0–2.6) was incubated at room temperature for ~15–20 min to allow complex formation. At final concentrations of ferritin (4 mg mL^{-1}) and chitosan (4–16 mg mL^{-1}) in the mixture, no visible precipitation/aggregation occurred during/after the mixing process. The pH of the formulation was adjusted to 2.5 and used for respective experiments as discussed in the sections below.

Gastric stability of bare and chitosan-fabricated apo and mineralized frog M ferritin

Native PAGE analysis of bare frog M ferritin. To investigate the impact of pepsin concentration and incubation period on the digestive stability of bare ferritin, *in vitro*, as-purified apo ferritin samples (1 mg mL^{-1}) were incubated in simulated gastric fluid (SGF; 100 mM glycine–HCl (pH 2.5)) with different concentrations of pepsin (0–5 mg mL^{-1}) at 37 °C for 1 h, 3 h and 6 h. In the course of incubation, all samples were constantly stirred at 150 rpm using an incubator shaker. Bare ferritin (1 mg mL^{-1}) at pH 7.0 (100 mM MOPS-NaCl) was taken as a control. The SGF treated samples were analysed on 5% native PAGE, and run at 100 V at room temperature using 25 mM Tris-glycine running buffer (pH 8.3).[18,47] The gels were then stained with Coomassie Brilliant Blue for visualisation of protein bands to analyse the cage integrity/assembly and protein degradation.[61,62]

Native PAGE analysis of chitosan-fabricated apo and mineralized frog M ferritin. Similarly, to study the impact of chitosan the apo and mineralized (~960 Fe/cage) ferritins were incubated in chitosan solutions at 1 : 1 ratio for 15–20 minutes (as discussed in the above section), prior to the digestive stability analysis. Bare and chitosan-fabricated apo and mineralized ferritin samples (1 mg mL^{-1}) were incubated in SGF at 37 °C for 1 h, 3 h and 6 h and run on native PAGE, as mentioned above for the apo-ferritin samples.[18,47] The iron retention ability of the bare and modified ferritin nanocages was analysed by visualising iron bands through the Prussian blue staining method. In brief as reported earlier, gels were incubated with a mixture of freshly prepared 2% $K_4Fe(CN)_6$ and 2% 11.6 M HCl (1 : 1, v/v) for appearance of the Prussian blue band.[47,61] The same gels were then washed with water and stained with Coomassie Brilliant Blue for visualisation of protein bands to analyse the degradation of ferritin protein and its cage integrity.

SDS–PAGE analysis

The SGF treated modified/unmodified apo-ferritin samples were analysed on 12.5% SDS PAGE, to investigate the digestive stability of ferritins (protein degradation pattern in gastric conditions) and the impact of chitosan on protein degradation. Prior to the experiments, SGF treated samples were prepared in SDS-denaturing buffer, with and without boiling, to understand the origin of secondary bands (in the absence of pepsin).

Transmission electron microscopy (TEM)

The mineralized ferritin (unmodified and modified) samples for TEM experiments were prepared similar to native PAGE (1 mg mL^{-1} ferritin samples were incubated under gastric pH 2.5 (100 mM Gly–HCl) and in SGF at 37 °C, and all samples were constantly stirred at 150 rpm using an incubator shaker). Sample grids were prepared as per our previous reports;[46,61] the 3 h incubated ferritin samples (5 μL) were poured onto a 300 mesh carbon-coated copper grid and negatively stained with 4% (w/v) gadolinium acetate tetra hydrate (uranyl acetate alternative) solution. Without delay samples were processed for TEM analysis (using an FEI Tecnai G2 TF30-ST transmission electron microscope equipped with a LaB_6 electron gun operating at 300 keV). The particle size distributions were obtained using ImageJ software.

Dynamic light scattering (DLS) and zeta potential analysis

The impact of chitosan on the gastric stability of bare and modified ferritin protein cages was investigated by measuring the hydrodynamic size using dynamic light scattering (DLS) (in a Malvern Zetasizer 90). Final concentrations of the ferritin samples were kept at 0.25 mg mL^{-1} and incubated with/without chitosan/pepsin in 100 mM Gly–HCl buffer (pH 2.5).

Identical samples (prepared in 10 mM MOPS-NaCl, pH 7.0, and 10 mM Gly-HCl, pH 2.5) were used for zeta potential analysis to investigate the surface charge of chitosan, bare-ferritin and chitosan–ferritin complex, using a clear disposable zeta cell (DTS1070) in a Malvern Zetasizer 90. Prior to DLS and zeta potential measurements, sample solutions were syringe filtered using a 0.22 μM PVDF membrane. All the measurements were performed at room temperature (25 °C).

Reductive and non-reductive iron release kinetics

Iron release from ferritins was performed by two different ways: reductive and non-reductive pathways. Prior to kinetic studies, the UV-Visible absorption spectra of Fe^{2+}/Fe^{3+}-chelator complexes were recorded by adding $FeSO_4$/$FeCl_3$ salts to chelator solutions in acidic and neutral buffer. λ_{max}, and molar absorptivity values were determined. The stoichiometries of iron to ligand (both Fe^{2+}-bipyridyl (bpy) and Fe^{3+}-deferiprone (DFP)) binding at neutral and gastric pH were determined using the continuous variation method (Job's plot). Iron and ligand concentrations were varied in the range of 0–1 mM (for Fe^{2+} and bipyridyl) and 0–0.5 mM (for Fe^{3+} and deferiprone) separately in 100 mM MOPS-NaCl (pH 7.0) and 100 mM gly-HCl buffer (pH 2.5). Throughout the iron release experiments the ferritin and pepsin concentration ratio was maintained at 1 : 1 in 100 mM Gly-HCl buffer (pH 2.5). Control iron release experiments were carried out in the 100 mM MOPS-NaCl buffer (pH 7.0).

Reductive iron release kinetics were initiated by adding 2.5 mM reducing agent, ascorbate and 1 mM Fe^{2+} chelator, bipyridyl, to unmodified and chitosan-fabricated mineralized ferritin (100 μM Fe) under the gastric condition. The $[Fe(Bpy)_3]^{2+}$ complex formed outside the ferritin cage was then quantified spectrophotometrically by monitoring the change in absorbance at 522 nm.[45,63,64]

Similarly, non-reductive iron mobilization kinetics were initiated solely by 400 μM of Fe^{3+} chelators (deferiprone (DFP) or deferoxamine (DFO)) from unmodified and chitosan-fabricated mineralized ferritin under the gastric condition. The kinetics of Fe^{3+} mobilization by DFP was obtained by monitoring the formation of the $[Fe(DFP)_3]$ complex at 513 nm (for pH 2.5) and at 455 nm (for pH 7.0). Similarly, the change in absorbance at 425 nm was monitored for iron release experiments by DFO at gastric pH.[65]

Circular dichroism (CD) analysis

The impact of gastric conditions and chitosan on the conformational/gastric stability of ferritin protein cages was investigated by monitoring far-UV CD spectra. CD of protein samples was measured with a spectropolarimeter (JASCO-1500) using a 2 mm cell.[64] Bare and chitosan-fabricated frog M ferritin was incubated in gastric pH 2.5 (100 mM Gly–HCl) or SGF for 3 h at 37 °C. Final concentrations of reaction components were as follows: ferritin (0.25 mg mL^{-1}–0.5 μM cage or 12 μM subunit), chitosan (0.25 mg mL^{-1}–1.0 mg mL^{-1}) and pepsin (0.25 mg mL^{-1}) with chitosan/ferritin (w/w) ratios ranging from 0 to 4 (equivalent to 0–40 chitosan per ferritin cage). The chitosan used in our report has a molecular weight (MW) of ~50.0 kDa and frog M ferritin has a MW of ~494.2 kDa.

Steady-state fluorescence analysis

The interaction of chitosan with ferritin and its impact on gastric stability (conformational changes due to denaturation/degradation) were investigated by analysing their intrinsic fluorescence properties. The sample solutions were prepared similar to CD analysis. The fluorescence emission spectra were scanned in the range of 290–550 nm with an excitation wavelength of 280 nm at 25 °C. The emission spectra of each sample were measured with a Fluoromax-4 spectrofluorometer (HORIBA Scientific) using a 10 mm path length quartz cuvette.

Results

Effect of gastric pH, pepsin concentration and incubation time on apo-ferritin cage integrity/stability

The stability of the frog M ferritin protein cage under gastric pH was studied *in vitro* by incubation in gly-HCl buffer (pH 2.5) to mimic the acidic environment of the stomach. Subsequently, the cage integrity of ferritin protein was analysed at different incubation periods (1 hour, 3 hours and 6 hours) by non-denaturing, native PAGE (Fig. 2). The density of the ferritin protein bands at pH 2.5 was found to be the same as that at neutral pH 7.0 (Fig. 2, L_1 and L_8), and no significant degradation was observed up to 3 hours of incubation. However, the band intensities were slightly lowered when the incubation period was extended to 6 hours, demonstrating that bare frog M ferritins can resist acid-catalysed cage-disintegration/degradation albeit partially losing their cage integrity with longer exposures.

In addition to hydrochloric acid, gastric juice has another critical component, pepsin, an endopeptidase, which breaks down the dietary proteins in the stomach. To investigate the action of pepsin on the structural stability of ferritin protein

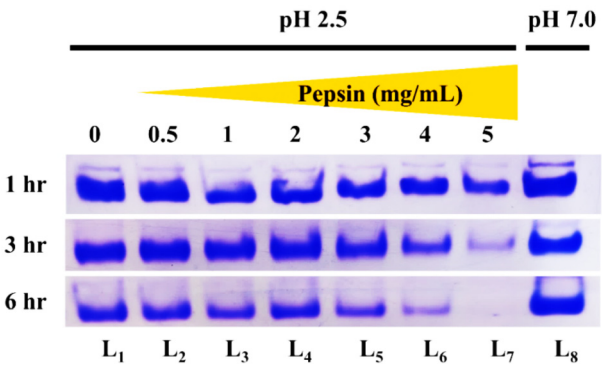

Fig. 2 Effect of gastric pH and pepsin concentration on the cage integrity of bare ferritin protein. Native PAGE analysis of the digestive stability of apoferritin against pH 2.5 and increasing concentration of pepsin (0–5 mg mL^{-1}; L_1 to L_7). Control (L_8): apo-ferritin sample at pH 7.0 in the absence of pepsin. Ferritin concentration was maintained at 1 mg mL^{-1} in the reaction solutions.

cages, frog M ferritin (1 mg mL^{-1}) was incubated in the simulated gastric fluid (SGF), with a range of pepsin concentrations (0.5–5 mg mL^{-1}) (Fig. 2). At 1 hour of incubation, ferritin protein samples exhibited an almost similar band intensity for lower pepsin concentrations. However, a progressive reduction in the band intensity was observed with the extension of incubation time. At higher pepsin concentrations of 5 mg mL^{-1} and 6-hour incubation time ferritin cages were completely disintegrated/degraded, indicated by the absence of protein bands (Fig. 2, L_7). This suggests that the stability of frog M ferritin protein cages is susceptible to denaturation/degradation under longer exposure to low pH and increased pepsin concentrations. Thus, unmodified (bare) frog M ferritins possess intrinsic structural stability, which allows them to withstand proteolytic digestion under physiological pepsin concentrations (0.5–1 mg mL^{-1})[66,67] at gastric pH 2.5 to a commendable extent.

Chitosan-decorated ferritin retains its cage integrity and iron bio-mineral under gastric conditions

As observed, unmodified frog M ferritin can resist gastric conditions to a certain extent where its cage integrity was influenced by pepsin concentrations and incubation time. To further improve its gastric stability, we fabricated apo-ferritins with chitosan. Native PAGE was carried out in order to investigate the impact of chitosan on ferritin cage-integrity (by Coomassie staining) and retention of encapsulated iron bio-mineral (by Prussian blue staining) in SGF (1 mg mL^{-1} pepsin at pH 2.5). A similar band intensity was seen for both apo and mineralized ferritin samples in the absence of pepsin (Fig. 3, L_1–L_4), which showed that the gastric pH had minimal effect on ferritin iron mineral dissolution. In the presence of pepsin, the cage integrity of the unmodified ferritin gradually weakens along with the loss of protein caged iron bio-mineral, as reflected in both its protein and iron-staining profiles (Fig. 3, L_5–L_6). Mineralized ferritins exhibited better cage integrity in comparison to their apo-form, possibly indicating the role of iron-mineral in cage stabilization.

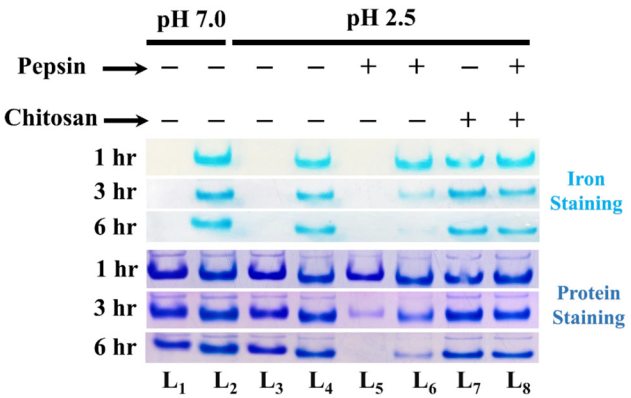

Fig. 3 Native PAGE analysis of digestive stability of the bare and chitosan-fabricated ferritin protein cage and its iron bio-mineral under gastric conditions. Apo-ferritin samples: L_1 (control), L_3 (control) and L_5; mineralized ferritin samples: L_2 (control), L_4 (control), L_6, L_7, and L_8. (+) and (–) signs represent the presence and absence, respectively, of chitosan and pepsin. Concentrations of ferritin, chitosan and pepsin were maintained at 1 mg mL^{-1} in the reaction mixture. Apoferritin and mineralized ferritin protein samples were run in a 5% (w/v) native gel at 100 V for 1.5 h and were treated with acidified $K_4Fe(CN)_6$ solution to visualize the encapsulated ferric iron mineral (by the formation of Prussian blue precipitate), followed by visualization of the ferritin protein cage *via* Coomassie staining.

However, chitosan-fabricated ferritins retained the cage-integrity and minimized the loss of encapsulated iron bio-mineral even in the prolonged incubation with pepsin (Fig. 3, L_7–L_8). This indicates that chitosan can protect the ferritin cage from degradation/disintegration while preserving the encapsulated bio-mineral under gastric conditions. The stabilizing effect of chitosan was further highlighted when its concentration was doubled (Fig. S2,† L_3 and L_7). This supports our idea that chitosan decorated ferritins would be efficient delivery vehicles for oral iron administration, allowing intact ferritins to traverse the gastric tract to reach the enterocytes.

Impact of chitosan on ferritin nanocage assembly under gastric conditions: TEM and DLS analysis

To investigate the impact of gastric conditions on the cage-assembly of bare and chitosan-fabricated ferritins, TEM analysis was employed for visualization of their microstructure and morphology. The ferritin protein sample at pH 7.0 (control) exhibited a clearly defined core–shell architecture for the protein cage and iron bio-mineral with average diameters of about 12 ± 1 nm and 5 ± 0.5 nm, respectively (Fig. 4A), as observed in our earlier reports.[46] When unmodified ferritin protein was incubated at pH 2.5, a similar size of mineral core was observed. This suggests that the ferritin protein coating stabilizes/protects the iron bio-mineral from dissolution/loss against acidic pH. Here, the lower visibility of protein cages may be because of the lower contrast provided by the negative staining agent (gadolinium acetate), possibly due to its altered interactions with the ferritin protein cage/background in acidic solutions (Fig. 4B).

However, both the core–shell morphology and the iron core were absent in pepsin treated bare ferritin samples (Fig. 4C). These disintegrated structures were fragile and prone to burn out under high electron beam energy (300 keV). In contrast to bare ferritins, the chitosan-fabricated ferritins were resistant to pepsin digestion and exhibited distinct cage and core structures (Fig. 4E). These findings well corroborate our native PAGE profiles.

Further, the dynamic light scattering (DLS) experiment was conducted to analyse the size distribution of both unmodified and chitosan-fabricated ferritin protein in aqueous buffer (Fig. 4F). Prior to the DLS experiment, samples were incubated under gastric conditions for 3 hours, except for the control (pH 7.0). In the absence of pepsin, at pH 2.5 bare ferritins are found to retain their cage assembly. However, the hydrodynamic size was apparently found to be higher in comparison to the control, possibly due to the loss of compactness of the

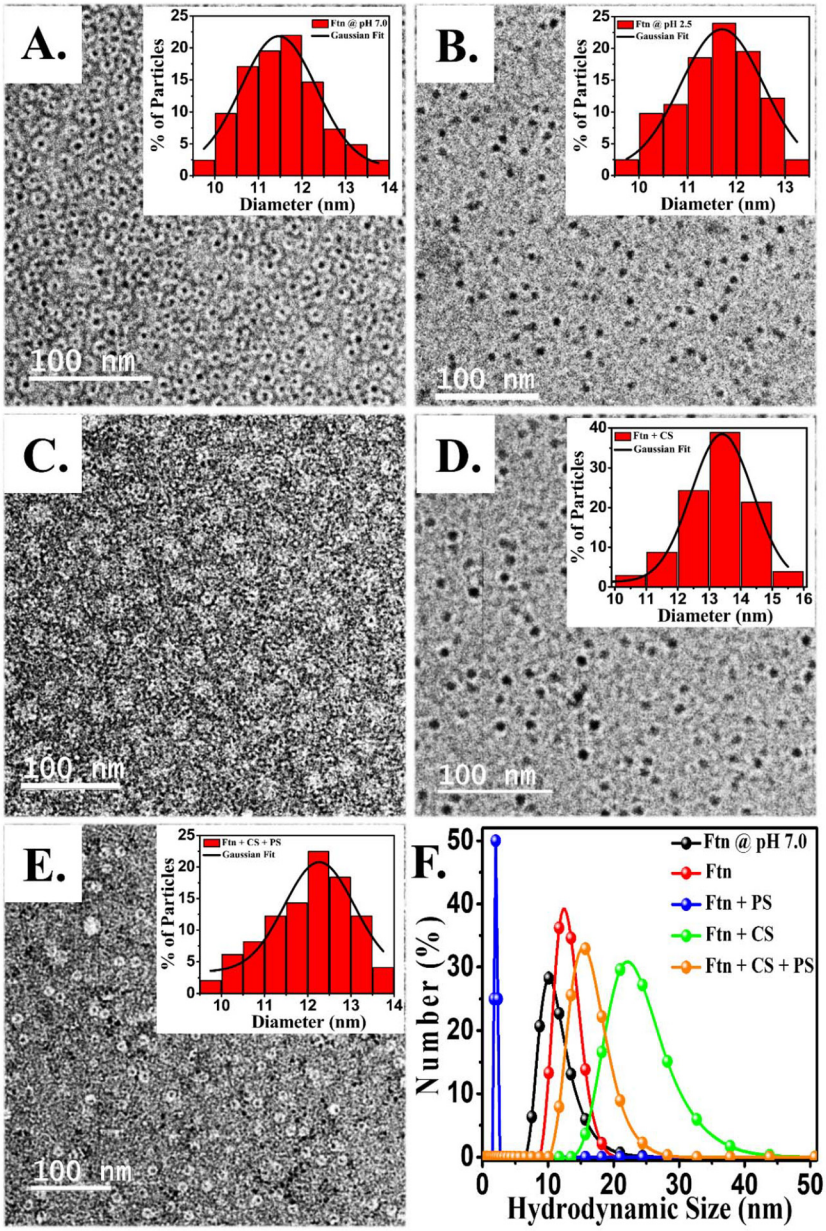

Fig. 4 Effect of gastric conditions on the cage assembly of unmodified and chitosan-fabricated ferritin samples. TEM images of (A) unmodified ferritin incubated at pH 7.0, (B) unmodified ferritin incubated at pH 2.5, (C) unmodified ferritin incubated with pepsin at pH 2.5, (D) chitosan-fabricated ferritin incubated at pH 2.5, (E) chitosan-fabricated ferritin incubated with pepsin at pH 2.5, and (F) their respective DLS based hydrodynamic sizes (diameter). All these biopolymers (ferritin: Ftn, chitosan: CS and pepsin: PS) were maintained at the same concentration *i.e.* 1.0 mg mL^{-1} and 0.25 mg mL^{-1} for TEM and DLS analysis, respectively. In panel F, all the samples were incubated at pH 2.5, except the control (in black).

protein structure in acidic buffer (faster protein breathing) (Table S1†).

But in the presence of pepsin, the size of unmodified ferritin was drastically reduced to ~2 nm, possibly due to the proteolysis induced disassembly. The increased hydrodynamic size of chitosan-fabricated ferritin (~24 nm) compared to unmodified ferritin (~15 nm) reflects ferritin–chitosan interaction (Table S1†). In the presence of pepsin, chitosan-fabricated ferritins possibly retain their assembly, unlike bare ferritins, which further supports our native PAGE and TEM analysis.

Surface charge analysis of bare and chitosan-modified ferritin by zeta potential study

The zeta potential was evaluated to investigate the surface charge of frog M ferritin protein, chitosan, and their complexes/intermolecular interactions. The zeta potential of ferritin nanoparticles was found to be negative (−8.9 ± 2.3 mV) at pH 7.0 and positive (+0.6 ± 1.5 mV) at pH 2.5 (Fig. 5). This data suggests a net negative and positive charge of the ferritin protein at pH 7.0 and 2.5, respectively, and correlates with the

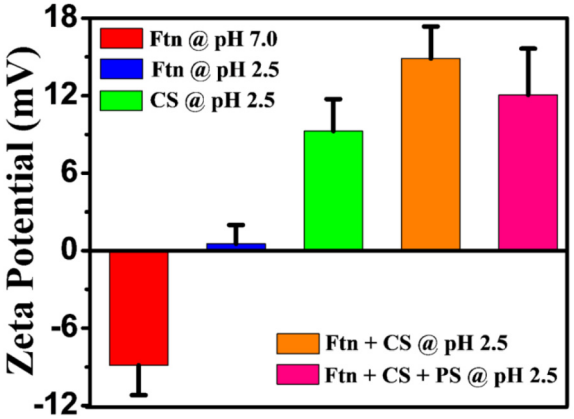

Fig. 5 Surface charge of ferritin, chitosan and their complex under gastric conditions. Zeta potential analysis for frog M ferritin, chitosan, and chitosan–ferritin complex by maintaining the same concentration *i.e.* 0.25 mg mL^{-1} in 10 mM Gly-HCl (pH 2.5). 10 mM MOPS-NaCl (pH 7.0) was used for neutral conditions. The data represents an average of three independent experiments and error bars indicate SD.

surface electrostatic potential data (APBS tool, Fig. S11†). Chitosan exhibited a positive zeta potential (+9.3 ± 2.5 mV) at lower pH 2.5, similar to earlier reports.[58,68]

As discussed in the methods section, the ferritin–chitosan complex was prepared by the addition of concentrated ferritin protein (pH 7.0) to chitosan (pH 2.5) in Gly-HCl buffer and the pH of the mixture was adjusted to 2.5 prior to zeta potential analysis. An increased zeta potential (+14.9 ± 2.5 mV) was observed at 1 : 1 w/w (~1 : 10 molar ratio) of ferritin : chitosan, which possibly indicates that ferritin–chitosan interactions are not predominantly electrostatic; rather, other interactions such as hydrophobic/H-bonding interactions may be involved. The higher positive zeta potential of the complex may be attributed to the outer layer *i.e.* chitosan, in contrast to reported Pickering emulsions with a ferritin outer layer.[69]

Degradation of bare and chitosan-fabricated ferritin under gastric conditions: SDS-PAGE analysis

To investigate whether chitosan–ferritin interaction could confer a protective effect on ferritin degradation against SGF, an SDS-PAGE based experiment was designed at 1 h, 3 h and 6 h incubation period similar to native PAGE. In SDS-PAGE non-covalent interactions between ferritin and chitosan are expected to be distorted during sample preparation (by the effect of SDS and boiling) and may migrate like bare ferritins, unlike previous reports on covalently modified ferritin.[70] However, it can be informative in providing the ferritin protein degradation pattern in gastric conditions and the impact of chitosan.

The purified frog M ferritin proteins exhibited a characteristic monomer band of ~21 kDa (Fig. 6, $\mathbf{L_2}$) and a high molecular weight band is also observed at the top possibly due to incomplete disassembly/denaturation at neutral pH. However, when incubated at pH 2.5, in the absence of pepsin, the bare ferritins showed secondary low molecular weight bands along with the monomer band (Fig. 6, $\mathbf{L_3}$). To validate whether these low molecular weight bands result from pH induced ferritin degradation (hydrolysis) or due to the boiling during sample preparation, we carried out two sets of experiments: with and without boiling (Fig. 6). When samples incubated at pH 2.5 were loaded into the SDS-PAGE without heating, only the characteristic monomer band was observed, indicating that the secondary bands may also result from the boiling step (Fig. 6, $\mathbf{L_6}$–$\mathbf{L_8}$). This suggests that proton induced/acid catalysed protein degradations are sensitive to temperature. Moreover, bare ferritin samples prepared without boiling (Fig. 6, $\mathbf{L_9}$) resist the cage disassembly/disintegration despite

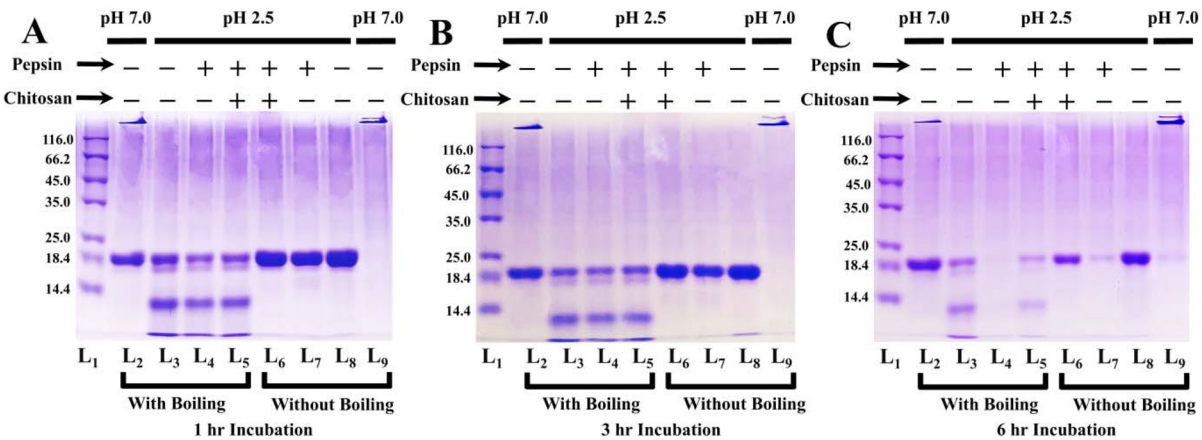

Fig. 6 Analysis of SGF treated bare and chitosan-fabricated ferritin degradation *via* SDS-PAGE. The fragmentation pattern of the bare and chitosan-modified ferritin complex in the presence and absence of pepsin at pH 2.5 analyzed with boiling (L_2, L_3, L_4, and L_5 samples were boiled for 15 min before loading) and without boiling (L_6, L_7, L_8, and L_9) for three different incubation periods: (A) 1 h, (B) 3 h, and (C) 6 h. L_2 and L_9 ferritin at pH 7.0 taken as the control. Concentrations of ferritin, chitosan and pepsin were maintained at 1 mg mL^{-1} in the reaction mixture. (+) and (–) signs represent the presence and absence of chitosan/pepsin. L_1: protein ladder. Under acidic conditions, the low molecular weight secondary bands may result from heating itself, in addition to the enzymatic activity of pepsin.

treatment with SDS and β-mercaptoethanol. This further indicates the chemical stability of the frog M ferritin cage where even the characteristic monomer bands were absent (Fig. 6, $\mathbf{L_9}$).

Upon treatment with pepsin, the intensity of the monomer band was gradually diminished due to ferritin degradation. Bare ferritin was able to sustain in the gastric condition up to 3 hours; a significant amount of cage was observed (Fig. 6B). However, the bare ferritins were almost completely degraded on incubation in SGF for 6 hours (Fig. 6C, $\mathbf{L_4}$ and $\mathbf{L_7}$). In contrast, chitosan-fabricated ferritin, in the presence of the pepsin enzyme, displayed a significant monomer band throughout the incubation period (Fig. 6, $\mathbf{L_5}$ and $\mathbf{L_6}$). This result confirms that chitosan is an effective protective agent for ferritin degradation in SGF and thus justifies its use as an enteric coating material.

Chitosan inhibits the reductive and non-reductive iron release from ferritin under gastric conditions

The TEM data correlates with native/SDS-PAGE and DLS analysis in establishing that chitosan helped ferritin to retain its cage integrity and protected the ferritin encapsulated iron mineral for an extended period of time. To further investigate the consequence of gastric conditions, presence of chelators and reducing agents in the digestive tract and the impact of chitosan, *in vitro* iron mobilization kinetics from mineralized ferritins (unmodified and modified) were studied following both reductive (using reducing agents and Fe^{2+} chelators) and non-reductive (using Fe^{3+} chelators) pathways.[71] Usually, the Fe-chelator complexes are formed outside the protein shell, which can then be quantified spectrophotometrically, based on their characteristic absorption properties. Prior to iron release kinetic experiments, the UV-visible absorption profile of Fe^{2+}/Fe^{3+}-chelator complexes was analysed by adding Fe-salts to chelator solutions in acidic and neutral buffer (Fig. 7A and B).

Fe^{2+} complexation of bipyridyl and the absorption behaviour of the $[Fe(Bpy)_3]^{2+}$ complex were found to be less sensitive to pH (Fig. 7A). The molar absorptivity was found to be 8.4 (±0.2) mM^{-1} cm^{-1} and 9.0 (±0.4) mM^{-1} cm^{-1} at 522 nm (metal to ligand charge transfer, MLCT-band) for pH 7 and 2.5, respectively (Fig. S4†), and binding stoichiometry was found to be 1 : 3 (metal:ligand) (Fig. 7C).

Reductive iron mobilization from mineralized ferritin (both unmodified/modified) was investigated *in vitro*, using ascorbate ($AscH^-$, a reducing agent) and bipyridyl (Bpy, a Fe^{2+} chelator). The amount of iron release from ferritin was quantified by monitoring the absorbance at 522 nm for the formation of the $[Fe(Bpy)_3]^{2+}$ complex. Iron release was significantly low at neutral pH (control reaction), possibly due to the compact protein structure and intact nanocage. Under gastric conditions, iron release exhibited a biphasic profile, a slow phase followed by a rapid phase, and release of a drastically higher amount of iron was observed as compared to the control (Fig. 7E). The higher iron release observed in bare ferritins under gastric conditions is possibly due to the following reasons: i. loss of their compact protein/pore conformation due to acidic pH, ii. pepsin activity, especially under longer incubation, and iii. the enhanced dissolution of iron mineral in the presence of reducing agents, iron chelators (which drive the complexation reaction) and acidic condition. This indicates that under gastric conditions, reducing agents and chelators may have a better access to the ferritin mineral core, facilitating higher iron release. However, when ferritins were modified with chitosan, iron release was significantly inhibited, possibly by retaining the compact nano-cage structure or by shielding ferritins against pepsin activity and low pH environment.

Similarly, prior to the non-reductive iron release experiments, the Fe^{3+}-deferiprone (DFP, a clinically used Fe^{3+} chelator) complex was characterized under both acidic and neutral conditions. Unlike $[Fe(Bpy)_3]^{2+}$, the absorption properties of the Fe^{3+}-DFP complex (possibly a mixture, $[Fe(DFP)_x]$) were pH sensitive, exhibiting different λ_{max} and molar absorptivities (Fig. 7B and Fig. S5†). The molar absorptivity was found to be 5.1 (±0.3) mM^{-1} cm^{-1} and 3.6 (±0.2) mM^{-1} cm^{-1} at 455 nm for pH 7 and at 513 nm for pH 2.5, respectively (Fig. S5†). Moreover, the binding stoichiometry was found to be different for the Fe^{3+}-DFP complex *i.e.* metal to ligand (~1 : 3) and (~1 : 2) at pH 7.0 and 2.5, respectively (Fig. 7D).

The iron mobilization kinetics from the ferritin core driven by the Fe^{3+}-chelator was studied by observing the change in the absorbance of the CT-bands of the Fe^{3+}-DFP complex at 455 nm and 513 nm (Fig. 7B). However, the non-reductive approach of iron mobilization from the ferritin core is remarkably slow as compared to the reductive approach possibly due to the low solubility of Fe^{3+} and stability of the ferrihydrite mineral core. Similar to the reductive approach, greater iron release was observed from bare ferritin, under gastric conditions, than the neutral conditions, possibly due to cage distortions caused by acidic pH and pepsin activity, enhancing mineral exposure to the chelating agents.

However, chitosan-fabricated ferritins retain a significant amount of iron even in the presence of pepsin and high affinity Fe^{3+} chelator. Similar iron release kinetic profiles were also observed when deferoxamine (DFO) was used as a Fe^{3+}-chelator (Fig. S6†). These results confirm that chitosan can effectively shield mineral loss from iron-loaded ferritins by minimizing cage disintegration/degradation and reducing agent/chelator accessibility under gastric conditions and thus may help iron release in a slow and controlled manner, to prevent iron-induced oxidative damage.

Chitosan retains the secondary structure of apo-ferritin under gastric conditions

The effect of gastric pH and pepsin on the structural integrity of bare ferritin protein and chitosan-fabricated ferritin protein samples has been examined using far-UV CD spectroscopy. Prior to the CD experiment, the bare and chitosan-fabricated apo ferritin proteins were incubated for 3 hours under gastric conditions. Far-UV CD spectra were acquired in the region 250 to 200 nm, to determine the secondary structures of ferritin

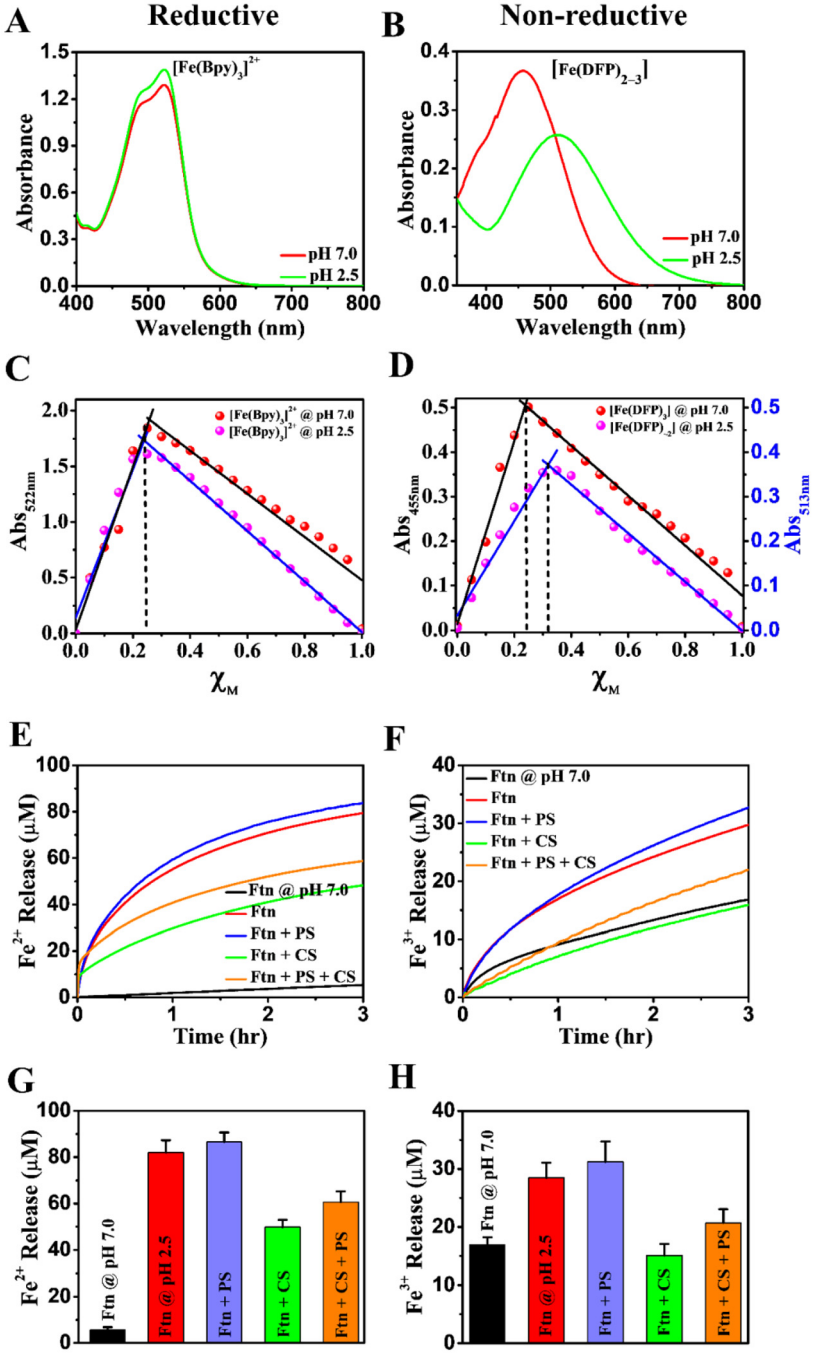

Fig. 7 pH dependent $Fe^{2+/3+}$-chelator complexation and effect of chitosan on reductive and non-reductive iron mobilization from ferritin under gastric conditions. UV-vis absorption spectra of (A) $[Fe(Bpy)_3]^{2+}$ and (B) $[Fe(DFP)_{2-3}]$ in neutral and acidic buffer. (C and D) Determination of binding stoichiometry for $[Fe(Bpy)_3]^{2+}$ and $[Fe(DFP)_{2-3}]$ complexes at pH 7.0 and pH 2.5 using Job's method. (E) Reductive iron mobilization facilitated by 2.5 mM ascorbate (as the reducing agent) and 1 mM bipyridyl (as the Fe^{2+} chelator). The kinetics of the $[Fe(Bpy)_3]^{2+}$ complex was recorded at 522 nm. (F) Non-reductive iron mobilization facilitated by deferiprone (DFP, Fe^{3+} chelator). The kinetics of Fe^{3+} mobilization was obtained by monitoring the formation of the Fe-DFP complex mixture at 513 nm (for pH 2.5) and at 455 nm (for pH 7.0). (G and H) Iron released after 3 hours of reductive and non-reductive kinetics. Iron release experiments were carried out in the 100 mM MOPS-NaCl (pH 7.0) and 100 mM Gly-HCl buffer (pH 2.5) using 0.2 μM bare/chitosan-fabricated mineralized ferritin (100 μM Fe). Experiments were replicated at least 4 times with 2 batches of purified protein preparations.

protein against the action of gastric pH and pepsin enzyme. Typically, bare ferritin exhibits two negative bands at 208 nm and 222 nm, which account for its α-helical nature (control reaction at pH 7, Fig. 8A).[47] At acidic pH 2.5, a partial loss (~20%) in the CD signal was observed for bare ferritin (Fig. 8A). This indicates that gastric pH has an influence on

the secondary structure of ferritin, despite retaining its cage integrity (as discussed in Fig. 2–4, PAGE, TEM and DLS data).

To validate chitosan–ferritin interaction and impact of chitosan on the secondary structure of ferritin, a range of chitosan concentrations (0.25 mg mL^{-1} to 1 mg mL^{-1}, prepared in Gly-HCl buffer pH 2.5) were titrated with a fixed concentration of ferritin (Fig. 8A). Increasing the concentration of chitosan recovers the CD signal, indicating its role in enhancing the stability/compactness of the ferritin protein against pH induced denaturation. The recovery of the CD signal appears to saturate at high molar ratios, possibly indicating the weak interactions between chitosan and ferritin at gastric pH (Fig. S8†).

For the pepsin treated unmodified ferritin protein samples (Fig. 8B), a drastic loss of the CD signal at 222 nm and 208 nm (α-helical signatures) suggests a significant denaturation/degradation of ferritin protein by the enzymatic action of pepsin. However, for the chitosan-fabricated ferritin protein, a substantial helical content is retained. Here we conclude that chitosan provides stability to ferritin protein and retains its helicity under gastric conditions.

Interaction of chitosan and ferritin under gastric conditions: steady-state fluorescence analysis

Protein fluorescence mainly arises due to the presence of intrinsic fluorophores (tyrosine and tryptophan). Their emission profile is sensitive to the microenvironment and thus provides information about the protein conformations and to a certain extent about protein denaturation/degradation. Therefore, steady-state fluorescence was recorded to study the stability of ferritin under gastric conditions and impact of chitosan on its denaturation/degradation process (Fig. 8C and D).

Before carrying out the measurement, the bare and chitosan-fabricated ferritin protein samples were incubated at the gastric pH in the presence and absence of pepsin for 3 hours. Bare ferritin at pH 7.0 (control) showed a strong fluorescence emission band at 330 nm upon excitation at 280 nm (Fig. 8C). At gastric pH 2.5, a decrease in intensity was observed for unmodified ferritins, without exhibiting an appreciable shift in the peak positions. This fluorescence quenching may be due to the enhancement in non-radiative pathways in the acidic environment. The increase in the acidity possibly does not alter the microenvironment of the fluorophore or the polarity of the medium significantly and thus, no major shift in the peak maxima was observed. The lone tryptophan (W89) is positioned on the BC loop which is on the external surface; therefore, increasing acidity may not alter the dielectricity of the aqueous buffer around the fluorophore (Fig. S10†). Upon titrating ferritin solutions (0.25 mg mL^{-1}) with varied concentrations of chitosan (0.25–1 mg mL^{-1}, prepared in Gly-HCl buffer pH 2.5), the fluorescence intensity was recovered similar to CD, further indicating its role in providing conformational stability/rigidity/protective coating against gastric pH.

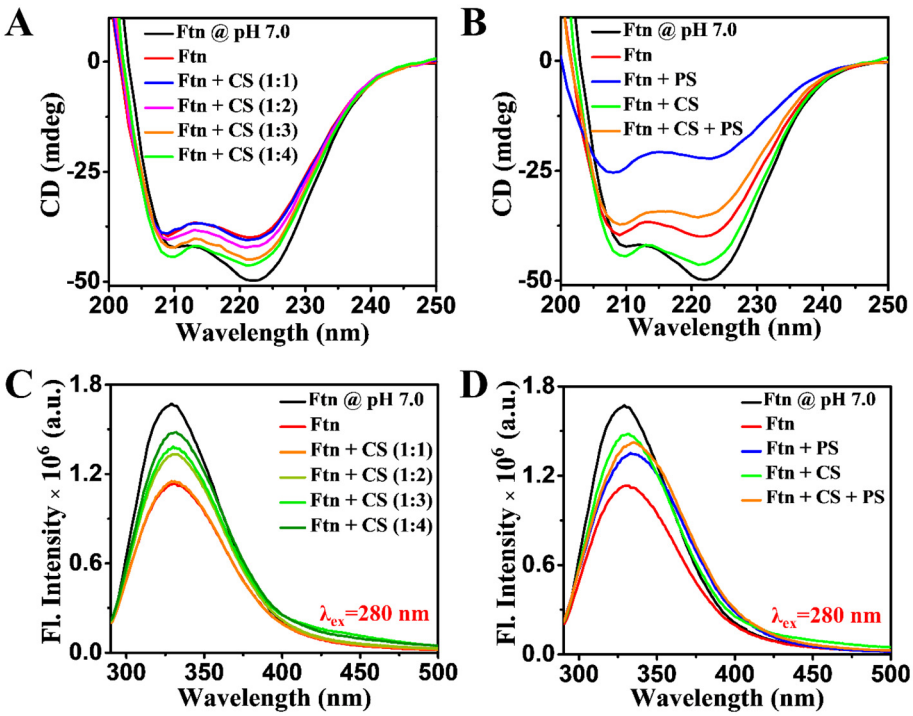

Fig. 8 Impact of chitosan on the secondary and tertiary structure of ferritin under gastric conditions. (A) Far-UV circular dichroism analysis of ferritin–chitosan interaction at a gastric pH of 2.5 (absence of pepsin). (B) CD analysis of pepsin treated bare and chitosan-fabricated ferritin. (C) Steady state fluorescence analysis of ferritin–chitosan interaction at the gastric pH 2.5 (absence of pepsin). (D) Fluorescence analysis of pepsin treated unmodified and chitosan-fabricated ferritin. The spectrum of bare ferritin protein at neutral pH 7.0 was recorded as a control. Contribution from only chitosan and only pepsin towards CD and fluorescence intensity has been corrected. All the samples were incubated at pH 2.5 for 3 hours, except the control (pH 7.0).

However, pepsin treated unmodified ferritin exhibited relatively lower fluorescence intensity compared to pH 2.5, possibly due to extensive protein degradation/denaturation by hydrolytic cleavage of pepsin. The quenching effects of gastric pH and pepsin on ferritin were further studied by using chitosan-fabricated ferritins (Fig. 8D). Here, chitosan recovers the ferritin fluorescence, by minimizing the conformational changes in gastric medium. However, within the experimental window (up to 0–40 molar ratios) fluorescence signal saturation was not observed (Fig. S8†), possibly due to weaker interactions between chitosan and ferritin under acidic conditions. The recovery of the signal upon chitosan titration at gastric pH is in contrast to earlier reports, where titration of chitosan to ferritin at circumneutral pH quenches the fluorescence intensity.[58,68] Moreover, the nature of binding and stoichiometry depends upon the size of the chitosan used, where higher MW chitosan may bind onto ferritin in a non-specific manner.[68]

Discussion

Anaemia is considered as a global public health issue associated with poor health outcomes due to the lack of sufficient normal red blood cells to meet physiological oxygen requirements.[1,2,5] It may have a variety of causes: nutritional deficiencies (inadequate intake of essential nutrients: iron, folate, vitamin B-12, *etc.*), genetic disorders (sickle-cell anaemia), thalassemia, chronic diseases (autoimmune disorders and cancer), and infections.[1] Iron deficiency anaemia (IDA) is the most prevalent one caused by insufficient iron in the body. The primary causes of IDA include inadequate dietary iron intake, malabsorption of iron or excessive blood loss. Typically, the best way to treat IDA is to replenish the body iron stores by supplementation with iron, either orally or intravenously.[72,73]

Intravenous (IV) iron supplementation provides a faster and direct route for retrieval of body iron stores, bypassing the gastric tract. However, it can cause discomfort at the injection site, as well as a risk of contracting infections (HIV/hepatitis) and other allergic reactions. Additionally, intravenous supplementations are relatively expensive and often require a medical professional for administration. In contrast to IV administration, oral administration is less expensive, non-invasive and requires minimal expertise, and thus it has been recommended as a convenient method for IDA treatment.[5,74]

The commercially available oral iron supplements are iron salts or complexes such as ferrous sulphate, ferrous gluconate, ferrous ascorbate, *etc.*, taken in the form of a "Fe^{2+} burst", which is associated with several side effects.[75] Free Fe^{2+} is oxidized by the O_2/H_2O_2 that generates ROS *via* the Fenton reaction and eventually leads to the formation of highly insoluble free Fe^{3+} (solubility 10^{-18} M at pH 7.0) that precipitates as Fe^{3+} oxide/hydroxide by complex hydrolytic chemistry. These cascades of oxidoreduction reactions may cause oxidative stress in the biological system, potentially leading to gastrointestinal upset. Moreover, precipitated Fe^{3+} species can accumulate in the gut, resulting in a decrease in absorption at the intestinal site (duodenal enterocytes). This readily available exogenous iron is easily accessible to pathogens (that may facilitate infection) and natural dietary inhibitors (phytates and polyphenols) of iron absorption.[9]

A major amount of micronutrient absorption occurs in the small intestine (enterocytes). Hence, an ideal oral iron supplement has to be able to sustain the micro-environment of the stomach and reach the site of absorption in an intact form, with nominal side effects. Ferritin protein encapsulated iron mineral was speculated to offer a potential solution to the issues associated with commercially available iron supplements. The slow and controlled release of iron from ferritin can potentially minimize the generation of ROS and non-transferrin bound iron (NTBI). Further, direct internalization of ferritin *via* receptor mediated pathways (TfR1, SCARA 5) would negate the interference of excess Fe^{2+} (iron-salt/supplements) on the dietary uptake of other essential nutrients (Cu^{2+} and Zn^{2+}) through DMT1. TfR1 expression is upregulated under iron deficiency condition,[76] which may help to meet iron requirements by facilitating higher ferritin uptake. Frog M ferritin shares almost 70% of sequence identity with human H ferritin; thus, frog M ferritin internalisation is expected to occur *via* the same TfR1 receptor as reported for H ferritin.[34] Therefore, the thermally and chemically stable frog M ferritins, with high iron storage efficiency, are proven as an ideal choice for iron supplementation.

Oral supplements need to pass through the stomach and reach the intestine (absorption site). The pH of the stomach in the upper digestive tract is nearly 1.5–3.0, in which the ferritin protein cage is expected to disintegrate/disassemble/degrade in addition to undergoing other secondary reactions (such as deamidation).[77] Interestingly, frog M ferritins, even in their bare form, were found to resist cage disintegration and loss of iron mineral, up to 3.0 hour of incubation (Fig. 2–4, PAGE and TEM data). In addition, frog M ferritin is relatively resistant to pH-mediated denaturation/degradation and retained its cage assembly (PAGE and TEM data, Fig. 2–4 and 6) despite exhibiting minor alterations in its hydrodynamic radii and conformational stability (DLS and CD). This corroborates some earlier reports on spleen and liver ferritin from horse and DNA binding protein from the starved cells (Dps) of *Listeria innocua*.[78] Our earlier reports on the kinetics of ferritin self-assembly have shown that frog M ferritin proteins can be disassembled into their subunits (assembly units) only below pH 2.0.[46] A slight increase in the hydrodynamic radii (cage swelling) was seen in frog M ferritin upon decreasing the pH from 7.0 to 2.5, possibly due to acid induced cage deformation/conformational changes. Drastic structural and conformational changes only occur under longer incubation and in the presence of pepsin. This indicates that iron loaded frog M ferritin can be used as a potential iron supplement in the solution form, requiring lesser gastric retention time, to reach the intestine in an intact form without much degradation. However, bare frog M ferritin protein cages were susceptible to denatura-

tion/degradation and loss of iron mineral under longer incubation in SGF (Fig. 3 and 4, PAGE and TEM data). These structural changes in ferritin possibly arise due to the acid induced disruption of inter and intra-subunit hydrogen bonds/electrostatic interactions, hydrolytic cleavage of peptide linkages and other non-covalent forces, which are responsible for maintaining the secondary, tertiary and quaternary structure of the ferritin protein cage. As a result of this degradation/disintegration process a significant amount of iron loss is observed, from the iron staining profiles (Fig. 3). Additionally, acceleration in mineral dissolution and mobilization is seen in the presence of chelators/reducing agents (Fig. 7).

Pepsin is an endopeptidase naturally adapted to function optimally in the highly acidic environment of the stomach. The reaction mechanism of this acidic protease involves two aspartate residues Asp-32 and Asp-215 and its catalytic efficiency is dependent on the reaction environment (pH 1.5–3.0),[79] the amino acid sequence and conformation of the target protein. Pepsin induced proteolysis may trigger the release of caged iron that may lead to adverse effects like commercially available iron salts. Therefore, it is necessary to further stabilize and protect the cage integrity and its caged iron from the harsh conditions in the stomach.

In this report we have chosen chitosan, an amine rich polycationic bio-polymer and food additive, to fabricate the ferritin surface to preserve its structural and functional features in the stomach environment. As envisioned, chitosan exhibited a greater impact on stabilizing ferritin cage integrity and preserving the encapsulated mineral in gastric conditions (Fig. 3). The fluorescence intensity/CD signal was recovered and the retention of the cage/caged iron was observed by PAGE, in the presence of chitosan. Similarly, both reductive and non-reductive dissolution and mobilization of ferritin mineral was significantly inhibited in the presence of chitosan, possibly by restricting chelator/reducing agent access to the iron mineral core. Opening and closing of ferritin pores can influence the kinetics of iron release.This has been observed earlier with pore alterations and in the presence of selected peptides and protein crowding agents.[63,80,81]

Chitosan, a food additive, is composed of three distinct types of nucleophilic functional groups, consisting of the $-NH_2$ group (at C-2 position, pK_a 6.3),[54] secondary –OH group (at C-3 position), and primary –OH group (at C-6 position) (Fig. 1), which allow it to interact with a variety of moieties at the ferritin surface. It has a high charge density (one positive charge per glucosamine residue) at gastric pH, which may favor electrostatic interactions with the negatively charged acidic amino acids (glutamate and aspartate) of ferritin protein. There are 32 acidic amino acids (19 glutamates and 13 aspartates) in a subunit of frog M ferritin protein, out of which about 18 are oriented towards the external surface, based on its crystal structure (PDB ID: 3KA3). Just on the basis of the theoretical pI ~5.6 of frog M ferritin sub-units, weak interactions with positively charged chitosan are anticipated due to the overall positive surface charge of ferritin at lower pH (Fig. S11†). However, as pK_a values are environment dependent, there is a possibility of lowering of pK_a values of carboxylate residues (side chains of glutamate and aspartate) of ferritins in the vicinity of ammonium ions $-NH_3^+$ (of chitosan) or basic amino acid residues: lysine, arginine, and histidine (of ferritin). In addition, the polar environment and the H-bonding to the deprotonated form of glutamate and aspartate ($-COO^-$) can also lower their pK_a values. For example, the average pK_a values of side chains of glutamate and aspartate residues in free amino acids/small peptides are ~4.2 and ~3.5, respectively, but based on the protein environment these pK_a values can shift to as low as 2.1 (for glutamate) and 0.5 (for aspartate).[59] Similarly for chitosan, the pK_a of $-NH_3^+$ (6.3) can increase significantly upon interaction with the negatively charged amino acids of ferritin. Under such circumstances, the electrostatic/charge–dipole interactions between the $-NH_3^+$ of chitosan and $-COO^-$ of ferritin get stabilized and can be a ferritin–chitosan binding possibility. However, the increased zeta potential of the ferritin–chitosan complex possibly suggests that ferritin–chitosan interactions are not primarily electrostatic. Therefore, there might be other stabilizing interactions such as H-bonding with the 1°, 2° –OH and hydrophobic interactions between chitosan and ferritins. These stabilizing interactions between chitosan and ferritins were previously reported at higher pH where electrostatic interactions were predominant.[58] This combined effect of these interactions helps the overall structural stability/cage integrity of ferritin, conferring better resistance against the gastric environment (low pH and protease activity). Other possibilities can be that chitosan forms a protective layer/shield around the ferritin protein, preventing the pepsin from coming in contact with ferritin or chitosan may compete with ferritin to interact with pepsin, shielding its proteolytic impact on ferritin. As hypothesized earlier, chitosan may interact with pepsin, either on its surface to block the substrate entry pathway or bind at the active sites (possibly with carboxylate residues)[82] to directly inhibit its enzymatic activity. As a result, the ferritin will be able to pass through the digestive system in its intact form without disintegration/digestion.

Since the last decade, cellular internalization of ferritin has remained an intense research interest in the field of iron metabolism and nano-biotechnology (targeted delivery of theranostic agents for imaging (MRI) and drugs (anti-cancer agents)).[26,32,83] H-ferritin has been extensively used for targeted drug-delivery and internalized through TfR-1 receptor mediated endocytosis. Previously, phytoferritins have been investigated for iron supplementation purpose using Caco-2 cell models.[37,84–86] Here we report a relatively acid stable protein cage in the form of bare and chitosan-fabricated frog M ferritin which can not only retain the protein cage but also preserve the iron mineral. A detailed understanding of molecular interactions between these enteric coating materials and ferritin protein will help to retain the cage and iron mineral (minimize iron induced toxicity/side effects) and can be a future prospective of this work. Moreover, it is reported that chitosan can facilitate cellular internalization of chitosan-fabricated ferritin loaded with cargo by both paracellular and

transcellular pathways.[68] It is also inferred that chitosan attachment did not obstruct the TfR1 binding site of ferritin and instead facilitated the transport of the ferritin *via* the TfR1-mediated endocytic pathway. However, we cannot negate the possibility that fabricating ferritin with chitosan may potentially mitigate recognition-based uptake mechanisms by altering surface properties and reducing the affinity for cellular receptors, which needs further investigation. Further, the mechanism of ferritin internalization (the receptors involved) and iron release pathways in enterocytes (NCOA4-mediated ferritinophagy, selective gating of ferritin pores, direct Fe^{3+} chelation or reductive pathway) are not well understood.[3,71,87] To have better insights into these prospects we aim to extend our work towards *in vivo* or cell line model studies as a future perspective.

Conclusion

In summary, we have explored the sustenance of unmodified and chitosan-fabricated frog M ferritins in gastric conditions to develop protein nanocage based iron delivery vehicles for effective oral iron supplementation with minimal side-effects. Our data suggests that, though frog M ferritins retain their cage assembly and caged-iron mineral up to 1–3 hours of incubation in low pH and pepsin mimicking gastric conditions, their cage integrity is compromised on longer incubation. Consequently, loss of iron mineral from the ferritin core was observed. Therefore, to ensure that iron-loaded ferritins cross the gastric tract in their intact forms, with minimal iron loss and limiting their access to pathogens or anti-nutrients, chitosan-fabricated ferritins were designed. Chitosan-fabricated ferritins showed both cage and mineral retention ability even at prolonged incubation time in SGF. The interactions between ferritin and chitosan were further validated. Chitosan inhibited iron mobilization from ferritin nanocages, possibly by limiting the access of chelating/reducing agents. Therefore, we anticipate that chitosan could potentially help ferritins to stabilize and further retain their bio-mineral content throughout the digestive tract. Our results hold promise for the development of an oral formulation based on bare and chitosan-fabricated frog M ferritin that can be a superior alternative for the treatment of IDA, offering targeted delivery and lower side effects. Further, this work on self-assembled ferritin protein nanocages may be extended towards co-encapsulation and delivery of iron with other bioactive nutrients.

Data availability

The data supporting this article have been included as part of the ESI.†

Conflicts of interest

There are no conflicts to declare.

Acknowledgements

This work was supported by Science and Engineering Research Board (SERB), India (CRG/2020/005332) and Science & Technology Department, Odisha, India (ST-SCST-MISC-0036-2023) to R. K. B. Authors are thankful to Prof. Elizabeth C. Theil (C.H.O.R.I., USA), for her generous support in providing the frog M ferritin clones and Dr Abhinav Mohanty and Prof. Usharani Subuddhi (NIT Rourkela, India) for their critical suggestions. We also appreciate Prof. Bismita Nayak and Mr Sanjiv Kumar (for DLS and zeta potential experiments) and Tanaya Subudhi for her experimental help.

References

1 WHO, *The global prevalence of anaemia in 2011*, World Health Organization, Geneva, Switzerland, 2015.
2 WHO, *Accelerating anaemia reduction: a comprehensive framework for action*, World Health Organization, Geneva, Switzerland, 2023.
3 E. C. Theil, T. Tosha and R. K. Behera, *Acc. Chem. Res.*, 2016, **49**, 784–791.
4 R. Crichton, in *Iron Metabolism: From Molecular Mechanisms to Clinical Consequences*, Wiley, 2016, p. 22.
5 C. Camaschella, *Blood*, 2019, **133**, 30–39.
6 K. Jimenez, S. Kulnigg-Dabsch and C. Gasche, *Gastroenterol. Hepatol.*, 2015, **11**, 241–250.
7 C. Camaschella and D. Girelli, *Mol. Aspects Med.*, 2020, **75**, 100861.
8 W. H. Koppenol and R. H. Hider, *Free Radical Biol. Med.*, 2019, **133**, 3–10.
9 N. Petry, I. Egli, C. Zeder, T. Walczyk and R. Hurrell, *J. Nutr.*, 2010, **140**, 1977–1982.
10 M. Abbas, Z. Hayirli, H. Drakesmith, S. C. Andrews and M. C. Lewis, *Front. Nutr.*, 2022, **9**, 927754.
11 C. Dehner, N. Morales-Soto, R. K. Behera, J. Shrout, E. C. Theil, P. A. Maurice and J. L. Dubois, *J. Biol. Inorg. Chem.*, 2013, **18**, 371–381.
12 A. Mohanty, B. Subhadarshanee, P. Barman, C. Mahapatra, B. Aishwarya and R. K. Behera, *Inorg. Chem.*, 2019, **58**, 4741–4752.
13 T. Richards, C. Breymann, M. J. Brookes, S. Lindgren, I. C. Macdougall, L. P. McMahon, M. G. Munro, E. Nemeth, G. M. C. Rosano, I. Schiefke and G. Weiss, *Ann. Med.*, 2021, **53**, 274–285.
14 E. C. Theil and R. K. Behera, Coordination Chemistry in *Protein Cages*, ed. T. Ueno and Y. Watanabe, John Wiley & Sons, Inc., 2013, ch. 1, p. 3.
15 E. C. Theil, R. K. Behera and T. Tosha, *Coord. Chem. Rev.*, 2013, **257**, 579–586.
16 F. Bou-Abdallah, *Biochim. Biophys. Acta*, 2010, **1800**, 719–731.
17 K. Honarmand Ebrahimi, P.-L. Hagedoorn and W. R. Hagen, *Chem. Rev.*, 2015, **115**, 295–326.

18 A. Parida and R. K. Behera, *Methods Mol. Biol.*, 2023, **2671**, 121–134.
19 N. D. Chasteen and P. M. Harrison, *J. Struct. Biol.*, 1999, **126**, 182–194.
20 A. Mohanty, A. Parida, R. K. Raut and R. K. Behera, *ACS Bio Med Chem Au*, 2022, **2**, 258–281.
21 E. C. Theil, *Nanotechnol. Perceptions*, 2012, **8**, 7–16.
22 E. C. Theil, *Inorg. Chem.*, 2013, **52**, 12223–12233.
23 B. Maity, K. Fujita and T. Ueno, *Curr. Opin. Chem. Biol.*, 2015, **25**, 88–97.
24 S. Abe, K. Hirata, T. Ueno, K. Morino, N. Shimizu, M. Yamamoto, M. Takata, E. Yashima and Y. Watanabe, *J. Am. Chem. Soc.*, 2009, **131**, 6958–6960.
25 M. Taher, B. Maity, T. Nakane, S. Abe, T. Ueno and S. Mazumdar, *Angew. Chem., Int. Ed.*, 2022, **61**, e202116623.
26 N. Song, J. Zhang, J. Zhai, J. Hong, C. Yuan and M. Liang, *Acc. Chem. Res.*, 2021, **54**, 3313–3325.
27 G. Jutz, P. van Rijn, B. Santos Miranda and A. Böker, *Chem. Rev.*, 2015, **115**, 1653–1701.
28 M. Uchida, S. Kang, C. Reichhardt, K. Harlen and T. Douglas, *Biochim. Biophys. Acta, Gen. Subj.*, 2010, **1800**, 834–845.
29 M. Khoshnejad, V. V. Shuvaev, K. W. Pulsipher, C. Dai, E. D. Hood, E. Arguiri, M. Christofidou-Solomidou, I. J. Dmochowski, C. F. Greineder and V. R. Muzykantov, *Bioconjugate Chem.*, 2016, **27**, 628–637.
30 J. W. Bulte, T. Douglas, S. Mann, R. B. Frankel, B. M. Moskowitz, R. A. Brooks, C. D. Baumgarner, J. Vymazal, M. P. Strub and J. A. Frank, *J. Magn. Reson. Imaging*, 1994, **4**, 497–505.
31 M. Khoshnejad, H. Parhiz, V. V. Shuvaev, I. J. Dmochowski and V. R. Muzykantov, *J. Controlled Release*, 2018, **282**, 13–24.
32 A. Kumar, B. Sharma and S. Lim, *Methods Mol. Biol.*, 2023, **2671**, 349–360.
33 L. Li, C. J. Fang, J. C. Ryan, E. C. Niemi, J. A. Lebron, P. J. Bjorkman, H. Arase, F. M. Torti, S. V. Torti, M. C. Nakamura and W. E. Seaman, *Proc. Natl. Acad. Sci. U. S. A.*, 2010, **107**, 3505–3510.
34 M. Liang, K. Fan, M. Zhou, D. Duan, J. Zheng, D. Yang, J. Feng and X. Yan, *Proc. Natl. Acad. Sci. U. S. A.*, 2014, **111**, 14900–14905.
35 L. C. Montemiglio, C. Testi, P. Ceci, E. Falvo, M. Pitea, C. Savino, A. Arcovito, G. Peruzzi, P. Baiocco, F. Mancia, A. Boffi, A. des Georges and B. Vallone, *Nat. Commun.*, 2019, **10**, 1121.
36 J. Y. Li, N. Paragas, R. M. Ned, A. Qiu, M. Viltard, T. Leete, I. R. Drexler, X. Chen, S. Sanna-Cherchi, F. Mohammed, D. Williams, C. S. Lin, K. M. Schmidt-Ott, N. C. Andrews and J. Barasch, *Dev. Cell*, 2009, **16**, 35–46.
37 C. D. San Martin, C. Garri, F. Pizarro, T. Walter, E. C. Theil and M. T. Nunez, *J. Nutr.*, 2008, **138**, 659–666.
38 B. Lonnerdal, A. Bryant, X. Liu and E. C. Theil, *Am. J. Clin. Nutr.*, 2006, **83**, 103–107.
39 J. F. Briat, C. Duc, K. Ravet and F. Gaymard, *Biochim. Biophys. Acta*, 2010, **1800**, 806–814.
40 E. C. Theil, *J. Nutr.*, 2003, **133**, 1549S–1553S.
41 G. Zhao, *Biochim. Biophys. Acta*, 2010, **1800**, 815–823.
42 A. Wang, K. Zhou and X. Qi, *Plant Foods Hum. Nutr.*, 2014, **69**(4), 386–391.
43 M. Hoppler, A. Schönbächler, L. Meile, R. F. Hurrell and T. Walczyk, *J. Nutr.*, 2008, **138**, 878–884.
44 D. Sala, S. Ciambellotti, A. Giachetti, P. Turano and A. Rosato, *J. Chem. Inf. Model.*, 2017, **57**, 2112–2118.
45 P. K. Koochana, A. Mohanty, S. Das, B. Subhadarshanee, S. Satpati, A. Dixit, S. C. Sabat and R. K. Behera, *Biochim. Biophys. Acta, Gen. Subj.*, 2018, **1862**, 1190–1198.
46 A. Mohanty, M. K. S. S. Jena and R. K. Behera, *Biomacromolecules*, 2021, **22**, 1389–1398.
47 B. Subhadarshanee, A. Mohanty, M. K. Jagdev, D. Vasudevan and R. K. Behera, *Biochim. Biophys. Acta, Proteins Proteomics*, 2017, **1865**, 1267–1273.
48 R. K. Behera and E. C. Theil, *Proc. Natl. Acad. Sci. U. S. A.*, 2014, **111**, 7925–7930.
49 R. K. Behera, R. Torres, T. Tosha, J. M. Bradley, C. W. Goulding and E. C. Theil, *J. Biol. Inorg. Chem.*, 2015, **20**, 957–969.
50 B. Chandramouli, C. Bernacchioni, D. Di Maio, P. Turano and G. Brancato, *J. Biol. Chem.*, 2016, **291**, 25617–25628.
51 Y. Kwak, J. K. Schwartz, S. Haldar, R. K. Behera, T. Tosha, E. C. Theil and E. I. Solomon, *Biochemistry*, 2014, **53**, 473–482.
52 I. C. C. Nóbrega, C. S. Ataíde, O. M. Moura, A. V. Livera and P. H. Menezes, *Food Chem.*, 2007, **102**, 186–191.
53 Y. Zhu, M. Bao, C. Chen, X. Yang, W. Yan, F. Ren, P. Wang and P. Wen, *Food Sci. Anim. Resour.*, 2021, **41**, 1049–1059.
54 M. N. Kumar, R. A. Muzzarelli, C. Muzzarelli, H. Sashiwa and A. J. Domb, *Chem. Rev.*, 2004, **104**, 6017–6084.
55 M. A. S. Abourehab, S. Pramanik, M. A. Abdelgawad, B. M. Abualsoud, A. Kadi, M. J. Ansari and A. Deepak, *Int. J. Mol. Sci.*, 2022, **23**(18), 10975.
56 S. K. Swain and A. Biswal, *Chitosan Nanocomposites*, Springer Singapore, 1 edn, 2023.
57 V. Mikušová and P. Mikuš, Advances in Chitosan-Based Nanoparticles for Drug Delivery, *Int. J. Mol. Sci.*, 2021, **22**(17), 9652.
58 R. Yang, Y. Gao, Z. Zhou, P. Strappe and C. Blanchard, *RSC Adv.*, 2016, **6**, 35267–35279.
59 C. N. Pace, G. R. Grimsley and J. M. Scholtz, *J. Biol. Chem.*, 2009, **284**, 13285–13289.
60 P. K. Koochana, A. Mohanty, A. Parida, N. Behera, P. M. Behera, A. Dixit and R. K. Behera, *J. Biol. Inorg. Chem.*, 2021, **26**, 265–281.
61 A. Parida, A. Mohanty, B. T. Kansara and R. K. Behera, *Inorg. Chem.*, 2020, **59**, 629–641.
62 A. Parida, A. Mohanty, R. K. Raut, I. Padhy and R. K. Behera, *Inorg. Chem.*, 2023, **62**, 178–191.
63 T. Tosha, R. K. Behera, H. L. Ng, O. Bhattasali, T. Alber and E. C. Theil, *J. Biol. Chem.*, 2012, **287**, 13016–13025.
64 A. Mohanty, A. Parida, B. Subhadarshanee, N. Behera, T. Subudhi, P. K. Koochana and R. K. Behera, *Inorg. Chem.*, 2021, **60**, 16937–16952.
65 J. Johnson, J. Kenealey, R. J. Hilton, D. Brosnahan, R. K. Watt and G. D. Watt, *J. Inorg. Biochem.*, 2011, **105**, 202–207.

66 H. Zhu, C. A. Hart, D. Sales and N. Roberts, *J. Med. Microbiol.*, 2006, **55**, 1265–1270.
67 A. Brodkorb, L. Egger, M. Alminger, P. Alvito, R. Assunção, S. Ballance, T. Bohn, C. Bourlieu-Lacanal, R. Boutrou, F. Carrière, A. Clemente, M. Corredig, D. Dupont, C. Dufour, C. Edwards, M. Golding, S. Karakaya, B. Kirkhus, S. Le Feunteun, U. Lesmes, A. Macierzanka, A. R. Mackie, C. Martins, S. Marze, D. J. McClements, O. Ménard, M. Minekus, R. Portmann, C. N. Santos, I. Souchon, R. P. Singh, G. E. Vegarud, M. S. J. Wickham, W. Weitschies and I. Recio, *Nat. Protoc.*, 2019, **14**, 991–1014.
68 R. Yang, J. Tian, D. Wang, C. Blanchard and Z. Zhou, *Food Funct.*, 2018, **9**, 2015–2024.
69 H. Chen, H. Dai, H. Zhu, L. Ma, Y. Fu, X. Feng, Y. Sun and Y. Zhang, *Food Hydrocolloids*, 2021, **126**, 107443.
70 X. Sha, Y. Zhang, Y. Li, R. Chen, H. Zhang, D. Meng, H. Chen and R. Yang, *J. Agric. Food Chem.*, 2024, **72**, 7464–7475.
71 N. Behera, G. Bhattacharyya, S. Behera and R. K. Behera, *J. Biol. Inorg. Chem.*, 2024, **29**, 455–475.
72 I. C. Macdougall, *Kidney Int. Suppl.*, 1999, **69**, S61–S66.
73 A. Kumar, E. Sharma, A. Marley, M. A. Samaan and M. J. Brookes, Iron deficiency anaemia: pathophysiology, assessment, practical management., *BMJ Open Gastroenterol.*, 2022, **9**(1), e000759.
74 C. Camaschella, *N. Engl. J. Med.*, 2015, **373**, 485–486.
75 F. Carmona, Ò. Palacios, N. Gálvez, R. Cuesta, S. Atrian, M. Capdevila and J. M. Domínguez-Vera, *Coord. Chem. Rev.*, 2013, **257**, 2752–2764.
76 K. Gkouvatsos, G. Papanikolaou and K. Pantopoulos, *Biochim. Biophys. Acta*, 2012, **1820**, 188–202.
77 N. E. Robinson and A. B. Robinson, *Proc. Natl. Acad. Sci. U. S. A.*, 2001, **98**, 12409–12413.
78 G. Bellapadrona, S. Stefanini, C. Zamparelli, E. C. Theil and E. Chiancone, *J. Biol. Chem.*, 2009, **284**, 19101–19109.
79 D. E. Beasley, A. M. Koltz, J. E. Lambert, N. Fierer and R. R. Dunn, *PLoS One*, 2015, **10**, e0134116.
80 C. M. Barnes, E. C. Theil and K. N. Raymond, *Proc. Natl. Acad. Sci. U. S. A.*, 2002, **99**, 5195–5200.
81 M. R. Hasan, T. Tosha and E. C. Theil, *J. Biol. Chem.*, 2008, **283**, 31394–31400.
82 T. Klein, U. Eckhard, A. Dufour, N. Solis and C. M. Overall, *Chem. Rev.*, 2018, **118**, 1137–1168.
83 M. Uchida, M. L. Flenniken, M. Allen, D. A. Willits, B. E. Crowley, S. Brumfield, A. F. Willis, L. Jackiw, M. Jutila, M. J. Young and T. Douglas, *J. Am. Chem. Soc.*, 2006, **128**, 16626–16633.
84 S. Bejjani, R. Pullakhandam, R. Punjal and K. M. Nair, *World J. Gastroenterol.*, 2007, **13**, 2083–2088.
85 C. Lv, G. Zhao and B. Lonnerdal, *J. Nutr. Biochem.*, 2015, **26**, 532–540.
86 A. Perfecto, I. Rodriguez-Ramiro, J. Rodriguez-Celma, P. Sharp, J. Balk and S. Fairweather-Tait, Pea Ferritin Stability under Gastric pH Conditions Determines the Mechanism of Iron Uptake in Caco-2 Cells, *J. Nutr.*, 2018, **148**(8), 1229–1235.
87 P. K. Koochana, A. Mohanty, B. Subhadarshanee, S. Satpati, R. Naskar, A. Dixit and R. K. Behera, *Dalton Trans.*, 2019, **48**, 3314–3326.